

# A Study on Calibration Methods for Infrared Focal Plane Array Cameras

Rasim Caner Çalik, Emre Tunali, Burak Ercan and Sinan Öz

Software Design Department, ASELSAN Inc. Microelectronics, Guidance and Electro-Optics Division, Ankara, Turkey

**Keywords:** Infrared Focal Plane Array, Non-uniformity Correction, Bad Pixel Detection, Bad Pixel Replacement.

**Abstract:** Imaging systems that are benefiting from infrared focal plane arrays (IRFPA) inevitably suffer from some visually unpleasant artifacts due to limits of detector materials and manufacturing processes. To address these artifacts and benefit the most from IRFPAs, factory level calibrations become obligatory. Considering nonlinear characteristics of infrared focal plane arrays, fixed pattern noise elimination, a.k.a. non-uniformity correction (NUC), and bad pixel replacement are considered as the most crucial calibration processes for capturing details of the scene. In this paper, we present two different NUC methods from two different families (temperature and integration time based NUC), together with a bad pixel detection strategy in order to achieve wide dynamic range and maximized contrast span.

## 1 INTRODUCTION

Infrared (IR) imaging systems are considered to be functional and fruitful in various military and civil applications (Gade and Moeslund, 2014). Even if change in detector types and technologies is a necessity for measuring radiation levels from different sections of IR spectrum, all IR imaging systems benefit from infrared focal plane arrays (IRFPA). IRFPAs consist of multiple independent detectors for scanning the scene in image pixel form. Although usage of FPA is a must for composing image, variations in characteristics of each individual detector yields different responses to unit change in IR radiation. The mentioned dissonance becomes apparent in form of spatial fixed pattern noise (FPN) and degrades radiometric accuracy, temperature resolution and quality of composed image (Milton et al., 1985). To compensate FPN, responses of all detectors must be calibrated in a way to achieve the same digital intensity level for the same amount of IR radiation and obtain the same effective response for unit change in radiation. This calibration is referred as non-uniformity correction (NUC). In NUC procedure, detector is assumed to have linear response (although it is not, see Figure 1) to achieve detector response characterization with two parameters, gain and offset, for each pixel. Model of detector response is described as follows:

$$S_{ij}(\phi) = K_{ij}\phi + Q_{ij} \quad (1)$$

where  $\phi$  represents digital value measured from incident flux on detector at  $i^{th}$  row and  $j^{th}$  column.  $K_{ij}$  is the gain coefficients of the characteristic curve and  $Q_{ij}$  is the offset coefficients.  $S_{ij}$  is the resultant image after NUC procedure. In other words, the goal of NUC procedure is to find  $K_{ij}$  and  $Q_{ij}$  such a way that each pixel should have the same effective response on unit change in thermal radiation yielding  $S_{ij}$  without any fixed pattern noise degradation.

Although NUC procedure achieves uniformity of pixels in general, usually some of the pixels (detectors) cannot follow the same response curve with others. These pixels generally have poor signal-to-noise ratio comparing to average pixels and referred as bad pixels. These pixels are observed in the composed image in form of saturated or flickering pixels; and can exist either individually or in cluster. As expected, these pixels are nothing but defects and should be detected and replaced to improve image quality. In order to achieve bad pixel replacement (BPR); a factory level bad pixel map (spatial locations of bad pixels) disclosed by bad pixel detection (BPD) procedures, together with a bad replacement scheme are required. Although literature includes various schemes for BPR; simple methods including nearest neighborhood (Isoz et al., 2005) and median algorithms (Celestre et al., 2016) are the most frequently used solutions in practice since BPR procedure should be conducted online. On the contrary, BPD schemes utilized as factory calibration and generally performed offline with

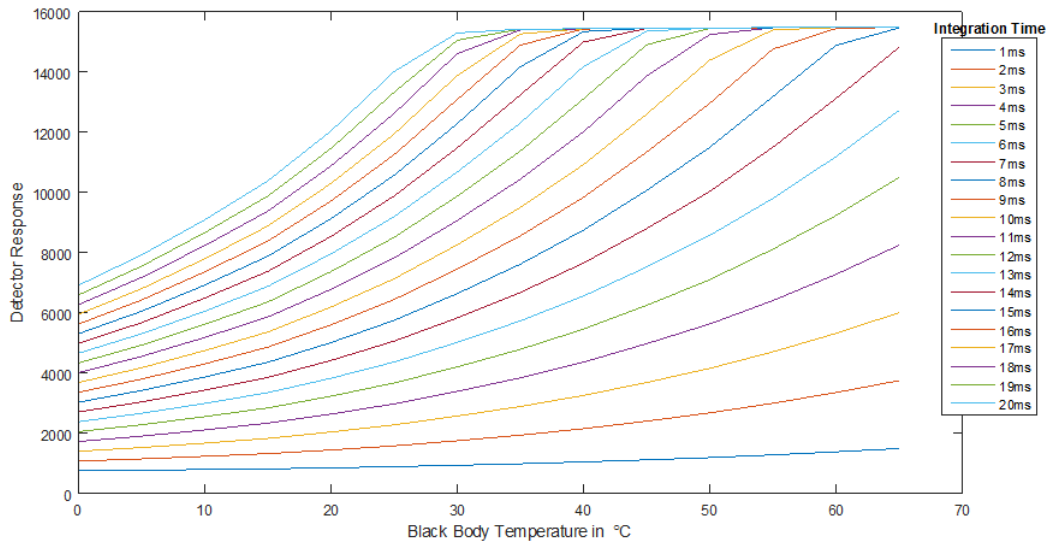


Figure 1: Exemplary Characterization Curves of Detector Illustrating Non-linearities.

more complex and iterative solutions.

For factory level calibration of IR imaging devices, this paper presents two calibration based NUC methodologies followed by an iterative bad pixel detection algorithm based on responsivity and NETD statistics of pixels. All procedures are tested on two different IRFPAs that are Sofradir MWIR MCT and QWIP (Altun et al., 2017) detectors. The remainder of the paper is organized as follows: First, we review related work in Section 2. Second, two different calibration methodologies are introduced in Section 3. Then, the experimental results are presented in Section 4, and followed by conclusions in Section 5.

## 2 RELATED WORK

Prior to operate any thermal imaging system on the field, essential calibrations including non-uniformity correction and bad pixel detection must be performed. Therefore, over the years, plenty of algorithms on non-uniformity correction and bad pixel detection are proposed in the literature.

### Non-Uniformity Correction (NUC)

NUC procedures are categorized into two families in the literature: calibration based (factory level) and scene based (run-time) algorithms. Despite their simplicity, calibration based methods generally achieves satisfactory results without the need of online coefficient calculation which is a critical advantage for real-time low power systems. To be more specific, this family estimates gain and offset values mentio-

ned in Eqn. 1 once through a calibration step at the factory and stores them into the system as tables. The most well-known and frequently used calibration based NUC methods are single point (Ness et al., 2017) and two point corrections (David L. Perry, 1993). In single point correction, a uniformly distributed radiation source is placed in front of IRFPA to estimate and update offset values in an existing NUC table. Details of single point NUC is given in Algorithm 1.

Two point correction achieves more successful results since it estimates both gain and offset coefficients of each pixel. For this estimation, two uniformly distributed radiation sources are required, generally two uniform IR blackbody sources at different temperatures. For each reference temperature, frame averages of collected image sequences are used to estimate gain-offset coefficients (David L. Perry, 1993).

Two point correction method can be extended to multi-point correction to interpret model non-linearity in terms of piecewise-linear functions; hence achieves

---

**Algorithm 1:** Single Point NUC Procedure.

---

**INPUT:** *ReferenceSet1*:  $imSet_1$ , maximum Offset:  $O_{max}$ , minimum Offset:  $O_{min}$

- 1:  $m_{sp1} = \text{mean2D}(imSet_1)$ ;
- 2:  $m_{sptmp1} = \text{mean}(m_{sp1})$ ;
- 3:  $o = \text{zeros}(m_{sp1}.height, m_{sp1}.width)$
- 4:  $rOff = m_{sptmp1}$ ;
- 5: **for**  $i = 1 : m_{sp1}.height$  **do**
- 6:     **for**  $j = 1 : m_{sp1}.width$  **do**
- 7:          $o(i, j) = rOff - m_{sp1}(i, j)$ ;
- 8:         **if** ( $o(i, j) > O_{max}$ ) **then**  $o(i, j) \leftarrow O_{max}$
- 9:         **if** ( $o(i, j) < O_{min}$ ) **then**  $o(i, j) \leftarrow O_{min}$

**OUTPUT:** *Offset Table*:  $o$

---

---

**Algorithm 2:** Two Point NUC Procedure.

---

**INPUT:**  $ReferenceSet1-2: imSet_1 - imSet_2, Max-Min$   
**Gain:**  $G_{max} - G_{min}, Max-Min Offset: O_{max} - O_{min},$

```

1:  $mSP_1 = mean2D(imSet1);$ 
2:  $mSP_2 = mean2D(imSet2);$ 
3:  $msptmp_1 = mean(mSP_1);$ 
4:  $msptmp_2 = mean(mSP_2);$ 
5:  $rGain = msptmp_1/msptmp_2;$ 
6:  $g = ones(mSP_1.height, mSP_1.width)$ 
7:  $o = zeros(mSP_1.height, mSP_1.width)$ 
8: for  $i = 1 : mSP_1.height$  do
9:   for  $j = 1 : mSP_1.width$  do
10:     $g(i, j) = rGain/(mSP_1(i, j)/mSP_2(i, j));$ 
11:    if  $(g(i, j) > G_{max})$  then  $g(i, j) \leftarrow G_{max}$ 
12:    if  $(g(i, j) < G_{min})$  then  $g(i, j) \leftarrow G_{min}$ 
13:  $rOff = msptmp_1;$ 
14: for  $i = 1 : mSP_1.height$  do
15:   for  $j = 1 : mSP_1.width$  do
16:     $o(i, j) = rOff - mSP_1(i, j) * g(i, j);$ 
17:    if  $(o(i, j) > O_{max})$  then  $o(i, j) \leftarrow O_{max}$ 
18:    if  $(o(i, j) < O_{min})$  then  $o(i, j) \leftarrow O_{min}$ 

```

**OUTPUT:** *Gain Table: g, Offset Table: o*

---

lower FPN (Young et al., 2008). However, this approach requires more data collection with more complex test setups during factory calibrations which reduces applicability. Although some other sophisticated calibration schemes achieving lower FPN levels exists (Milton et al., 1985; David L. Perry, 1993; Yuan et al., 1995; Schulz and Caldwell, 1995; Jonah C. McBride, 2009), generally they are not preferred due to their long and costly calibration processes.

As mentioned previously, second family for FPN elimination is referred as scene based NUC (Vera et al., 2011; Liang et al., 2014; Kumar, 2013). They are based on one simple fact, scene and fixed pattern noise is uncorrelated. Scene-based techniques calculate gain and offset values at each frame by exploiting motion-related features in image sequences online which restricts usage of this family for some applications. Since we are more focused on calibration techniques for low-power thermal imaging systems, calibration based NUC methods fit better for our purposes rather than scene based approaches.

### Bad Pixel Detection and Replacement

After NUC procedure, some of the pixels does not behave as expected and produces abnormal values. Therefore, data provided by these pixels can be considered as completely useless or less reliable than the data produced by its neighboring pixels. For many applications, imaging system should be able to correct bad pixels without disturbing informative parts of image.

This could be achieved by generating a binary map for bad pixels and performing replacement by obtaining data from neighboring pixels.

Usage of two point NUC table coefficients is one of the simplest method for bad pixel detection. In (Lin and Calarco, 1990), pixels whose gain or offset values are outside of the expected ranges are labeled as bad pixels. In (Celestre et al., 2016), bad pixel map is generated based on linearity as a function of integration time. First, multiple images are taken at a specific integration time then integration time is increased step by step until saturation of the detector is reached. From this data, "coefficient of determination" is calculated as explained in (Anderson-Sprecher, 1994) and compared with a threshold to label bad pixels. In median spatial spectral based algorithm, (Amber D. Fischer, 2007), the ratio of the corresponding and neighboring pixels is controlled. If this ratio is much less or much more than an expected value, this pixel is marked as bad pixel.

For bad pixel replacement, proposed methods usually benefits from neighboring pixels. For this purpose, nearest neighbor (Isoz et al., 2005), median (Celestre et al., 2016) and interpolations (Kai et al., 2016) are the most common replacement methods. Nearest neighbor is the most simple form of replacement algorithms which uses nearest healthy pixel value for replacing bad pixel. Median method is also similar and selects single pixel value for replacement as the median of neighboring pixels. In interpolation algorithms bad pixels are replaced by weighted average of neighboring pixels instead of a single pixel value.

## 3 METHODOLOGY

### 3.1 Temperature and Integration Time based Non-Uniformity Correction

Any IR imaging system aims to have wide linear dynamic range while maintaining maximum contrast span. However, these two requirements can be conflicting. Wide dynamic range is related with simultaneously and successfully responding low and high level radiation sources at the scene (objects at low and high temperatures together); whereas contrast span is about responsivity which is aimed to respond unit change in radiance as high as possible to extract more details of the target. Actually, selection of which parameters to modulate for calibration, either integration time (IT) or temperature, determines which interest to be favored more. IT based methods are expected to be more effective if the temperature span of the scene is

**Algorithm 3:** NETD Based BPD Procedure.

**INPUT:** *ReferenceSet1-2: imSet<sub>1</sub> – imSet<sub>2</sub>, Reference Temperatures: T<sub>1</sub> – T<sub>2</sub>, Max-Min Offset: maxOff – minOff*

```

1: respMap = mean2D(imSet1) – mean2D(imSet2);
2: respAvg = mean(respMap)
3: resp1K = respMap/(T1 – T2)
4: fpnlm1 = std(avgFrame1)
5: NETD = fpnlm1/resp1K
6: netdTh = 1
7: for i = 1 : MaxIterationCount do
8:   netdThPrev = netdTh
9:   avgNETD = 0
10:  validPxlCnt = 0
11:  for y = 0 : im1.height do
12:    for x = 0 : im1.width do
13:      pxlNETD = NETD(y,x)
14:      if pxlNETD > netdTh then
15:        bpdMap(y,x) = 1
16:      else if pxlNETD > 0 then
17:        avgNETD+ = pxlNETD
18:        validPxlCnt+ = 1
19:      avgNETD = avgNETD/validPxlCnt
20:      netdTh = avgNETD*3
21:      if abs(netdTh – netdThPrev) == 0 then
22:        break

```

**OUTPUT:** *Bad Pixel Map: bpdMap*

in the vicinity of the reference temperature utilized in NUC. Obviously, that is a limiting constraint which restricts their usage in complex scene. To achieve IT based NUC, two image sequences are collected from a blackbody on fixed temperature in two different integration times. Frame averages are calculated for each integration time to estimate reference gain, which indicates average responsivity between two integration times. After calculating gain coefficients for all pixels, one of the image set is selected to calculate offsets. Details on gain offset table calculation is given in Algorithm 2.

For temperature based method, the same procedure is followed. Instead of changing integration time, temperature of the blackbody is changed a integration time fixed. More than one gain offset tables can be obtained by changing temperature of blackbody for different integration times to optimize wide dynamic range with better contrast stretch.

### 3.2 Bad Pixel Detection

Sensor quality assessment metrics are closely related with bad pixel detection since they are designed to measure wellness of each pixel. Responsivity and Noise Equivalent Temperature Difference

(NETD) metrics can be considered as two crucial metrics.

Responsivity (R), (Shi et al., 2009), measures the change of detector response to a unit temperature change; hence it is a critical performance metric.

$$R = \frac{\Delta DigValue}{\Delta T} \quad (2)$$

Here,  $\Delta T$  is the temperature change of the blackbody image, and  $\Delta DigValue$  is the defined as digitized detector response change. Hence, pixels having significantly lower or higher than average responsivity cannot be considered as healthy pixels.

NETD, (Wang et al., 2015), is another measure for how well designed for defining the noise characteristic of the IR focal plane arrays by measuring temporal noise. NETD is typically measured in milliKelvin(mK) and obtained by following the steps:

1. Take N images @T°K blackbody and calculate the standard deviation of the image (noise characteristic).
2. Calculate the temporal average for N images and assign this image as AVGTK.
3. Take N images @T+ $\Delta T$ °K blackbody
4. Calculate the temporal average for N images and assign this image as AVGT2K.
5. Subtract AVGTK from AVGT2K to obtain R response map.
6. Divide R response by  $\Delta T$  to obtain 1K change response map.
7. Divide the noise by the 1K change map to obtain the NETD map

We benefited from responsivity and NETD characteristics of the sensor, in order to disclose bad pixel map. For measuring these characteristics image sequences obtained from blackbody during NUC procedures are used. Details of the bad pixel detection procedure is elaborated in Algorithm 3.

For bad pixel replacement, median algorithm proposed in (Celestre et al., 2016) is utilized.

## 4 EXPERIMENTAL RESULTS

To compare performance of two different NUC algorithms, a series of experiments were repeated for two different detectors that are Sofradir MWIR MCT and QWIP. Both detectors produces 14-bit digital outputs and has same pixel resolution and dimensions, 640 x 512 and 15  $\mu\text{m}$  x 15  $\mu\text{m}$  respectively. An SR-800N Extended Area blackbody with emissivity of

Table 1: Sofradir MWIR MCT Test Results.

Integration Time (ms)	Temperature (°C)	Raw Image	Temp. Based	IT Based
3	15	6.4302	0.6574	0.4838
	30	5.7847	0.4701	0.2300
	45	5.6460	0.3312	0.1026
	60	5.7132	0.2398	0.1647
5	15	5.5021	0.1652	0.5111
	30	5.5368	0.0932	0.2168
	45	5.7167	0.0818	0.0818
	60	5.9024	0.0953	0.1653
7	15	5.3116	0.3495	0.5401
	30	5.5607	0.2284	0.2363
	45	5.7968	0.1816	0.1065
	60	5.9613	0.1919	0.1792

0.97 ± 0.02 was used. Blackbody is located approximately 15 cm away from detectors. For Sofradir detector, data was collected at integration times 3 ms, 5 ms, 7ms and temperatures 15°C, 30°C, 45°C, 60°C as the sampling points. For QWIP, data points are picked from integration times 10 ms, 16 ms, 22 ms and from temperatures 10°C, 20°C, 30°C, 40°C. After collection of raw data at specified sample points, this data processed by first using either IT or temperature based NUC then bad pixels are corrected. For Sofradir detector, two point NUC is achieved for IT based method by using data of 45°C with 3ms and 5 ms integration times; whereas temperature based NUC is performed for fixed 5ms integration time with 30°C and 45°C temperature samples. For QWIP detector, IT based NUC is utilized at integration time 10ms and 16ms at 30°C, while temperature based NUC is achieved for 16ms integration time with 10°C and 30°C. To compare performances of different NUC results, well-known non-uniformity parameter (NU) is adopted from (Godoy et al., 2008) is given in Eqn. 3.

$$NU = \frac{1}{\bar{I}} \sqrt{\frac{1}{M \times N - d} \sum_{i=1}^M \sum_{j=1}^N (I_{ij} - \bar{I})^2} \times 100\%, \quad (3)$$

$$\bar{I} = \frac{1}{M \times N - d} \sum_{i=1}^M \sum_{j=1}^N I_{ij}$$

where  $\bar{I}$  is the average gray value of all pixels, omitting the bad pixels which are numbered as  $d$ , and  $I_{ij}$  is the gray value of the pixel at  $i^{th}$  row and  $j^{th}$  column.  $M \times N$  is the number of total pixels in IRFPA. It should be noted that lower NU scores indicate better uniformity (NUC results). NU metrics are evaluated for each detector for different integration times and scene temperatures are summarized in Table 1 and 2.

Examining the results, it is observed that IT based approach always yields minimum NU values for the scenes with low temperature difference from which NUC is performed. As temperature difference increases, NU scores of IT based approach rapidly in-

Table 2: QWIP Test Results.

Integration Time (ms)	Temperature (°C)	Raw Image	Temp. Based	IT Based
10	10	10.0483	3.7559	0.8273
	20	10.1154	3.5250	0.3949
	30	10.1621	3.1674	0.1290
	40	10.2463	2.8281	0.3883
16	10	9.4335	0.0991	0.7951
	20	9.5618	0.1087	0.3756
	30	9.6802	0.0846	0.084
	40	9.8297	0.1016	0.3727
22	10	9.2234	1.6141	0.7695
	20	9.3714	1.4539	0.3681
	30	9.5208	1.3727	0.1728
	40	9.7192	1.2834	0.4709

creases; which shows susceptibility of IT methods to temperature differences. On the contrary, if scene includes radiation sources that diverge from NUC reference temperature, temperature based calibration scores stay more stable for relevant integration times.

Figure 2 and 3 includes scenes with different temperature span and supports previous findings visually. At each figure, left column includes outputs of temperature based NUC whereas right column illustrates IT based results. As it can be seen, Figure 2 includes a scene having tight temperature span around 37°C, while Figure 3 is mainly around 25°C and has an extra target at 15°C. Since in Figure 2, scene temperature is close to NUC temperature, both method achieves successful results, IT is slightly better. However, when temperature of the scene is not close the NUC temperature, performance of IT based NUC deteriorates, see Figure 3. Considering these results, generation of multiple NUC tables by using IT based NUC for various temperatures could be a method for calibration. If these tables could be switched while performing online operating mode, high dynamic range could be achieved with a good contrast span.

## 5 CONCLUSIONS

For effectively using any infrared thermal imaging system in the field, factory level NUC and BPD calibrations are compulsory. Moreover, performance of these calibrations are directly correlated with the quality of composed image which is equivalent to quality of imaging system as a final product. In this paper, we studied on calibration strategies to achieve IR imaging systems having wide linear dynamic range and contrast span simultaneously.

Considering the experimental results, we observed that generation of multiple NUC tables by using IT based NUC for different temperatures could be a method for calibration. If these tables could be switched during online operation, high dynamic range could be achieved with a good contrast span.

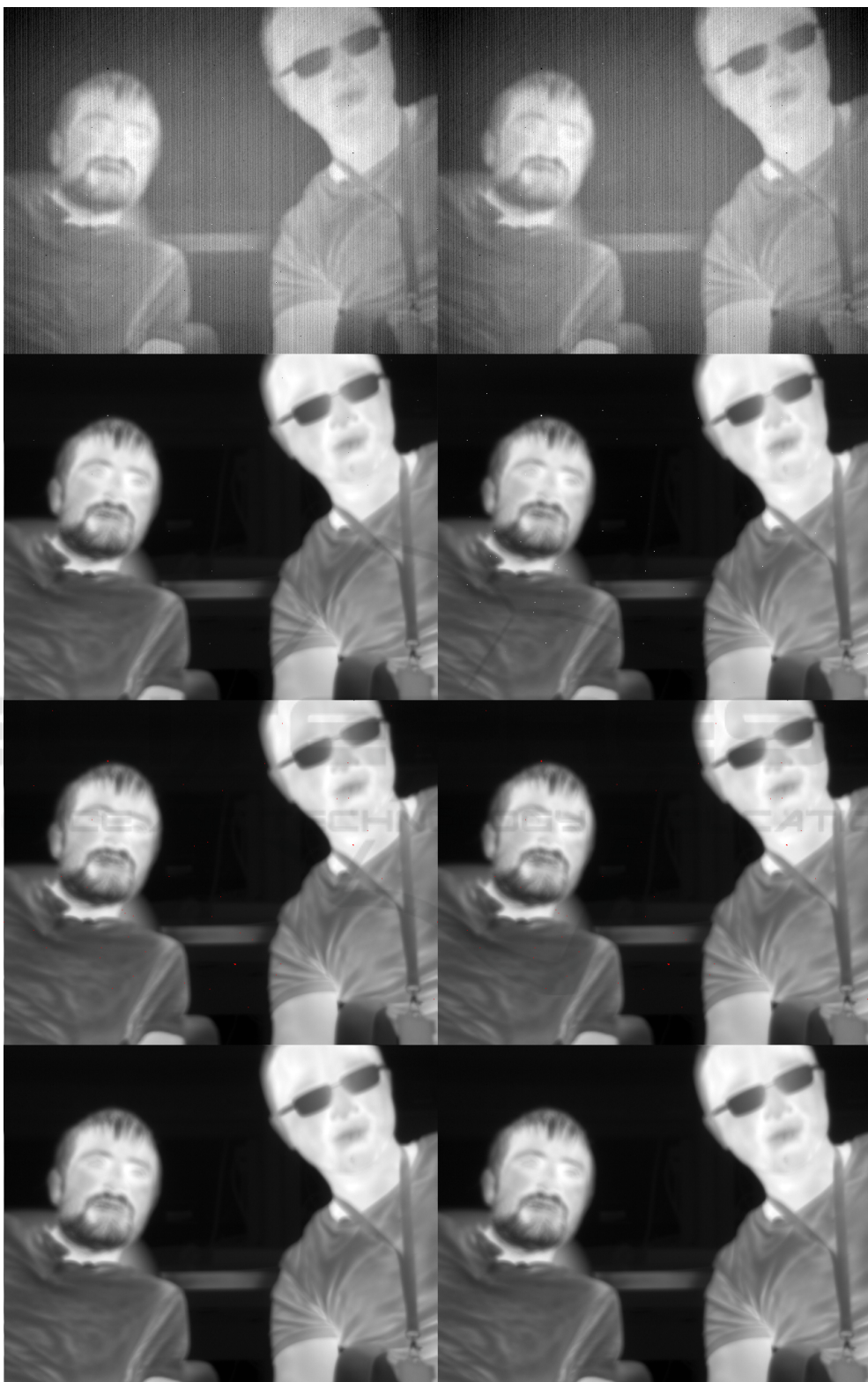


Figure 2: Left column includes outputs of temperature based calibration while right column illustrates integration time based results. Rows demonstrates from top to bottom: raw data, output of performed NUC, bad pixel map (marked with red), and final calibration result.

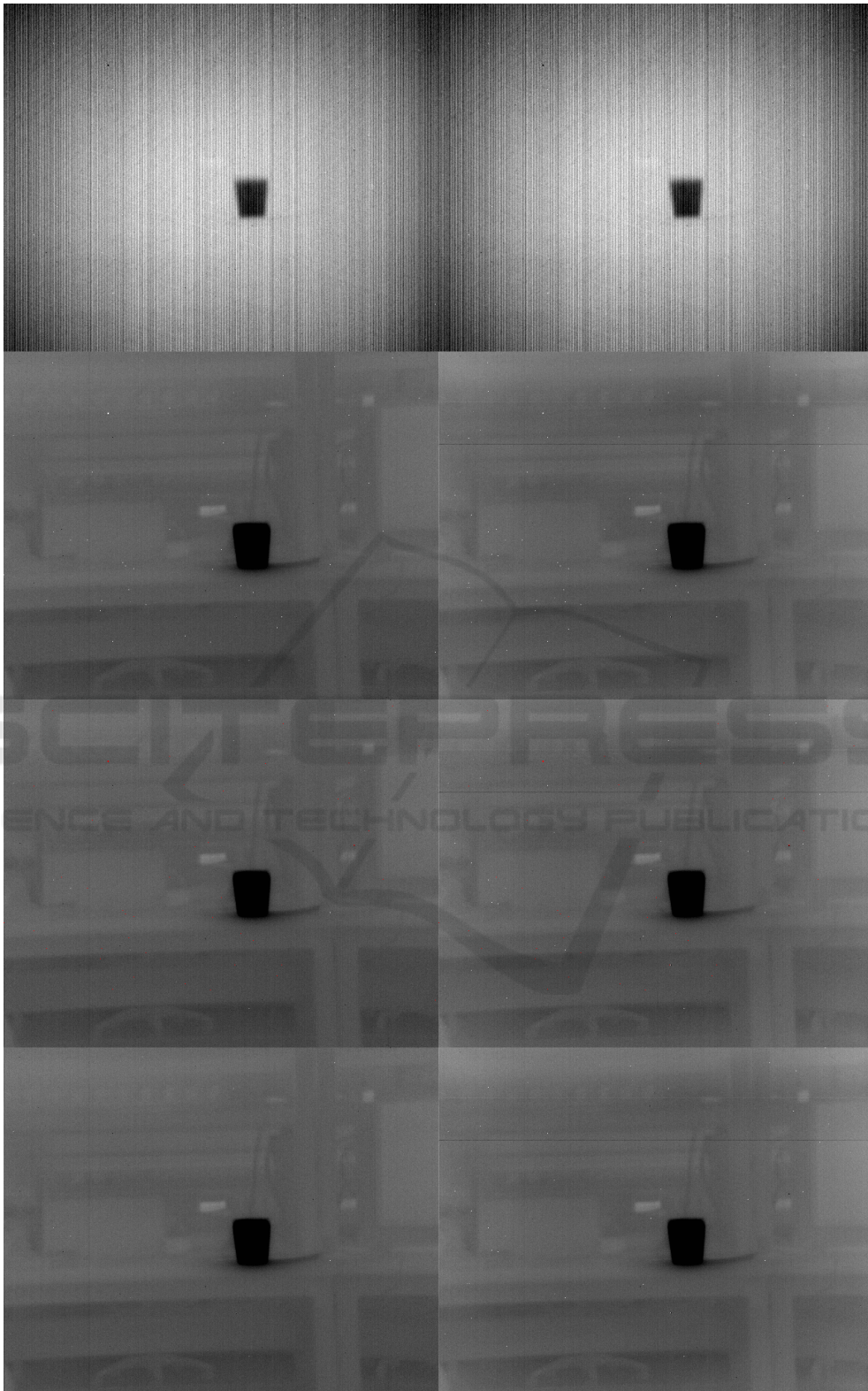


Figure 3: Left column includes outputs of temperature based calibration while right column illustrates integration time based results. Rows demonstrates from top to bottom: raw data, output of performed NUC, bad pixel map (marked with red), and final calibration result.

## REFERENCES

- Altun, O., Kepenek, R., Tasdemir, F., Akyurek, F., Akbulut, C. T. M., Nuzumlali, O. L., and Inceurkmen, E. (2017). Development of a fully programmable roic with 15  $\mu\text{m}$  pixel pitch for mwir applications.
- Amber D. Fischer, T. V. Downes, R. L. (2007). Median spectral-spatial bad pixel identification and replacement for hyperspectral swir sensors.
- Anderson-Sprecher, R. (1994). Model comparisons and r2. *The American Statistician*, 48(2):pp. 113–117.
- Celestre, R., Rosenberger, M., and Notni, G. (2016). A novel algorithm for bad pixel detection and correction to improve quality and stability of geometric measurements. *Journal of Physics: Conference Series*, 772(1):012002.
- David L. Perry, E. L. D. (1993). Linear theory of nonuniformity correction in infrared staring sensors. *Optical Engineering*, 32:32 – 32 – 6.
- Gade, R. and Moeslund, T. B. (2014). Thermal cameras and applications: a survey. *Machine Vision and Applications*, 25(1):245–262.
- Godoy, S. E., Pezoa, J. E., and Torres, S. N. (2008). Noise-cancellation-based nonuniformity correction algorithm for infrared focal-plane arrays. *Appl. Opt.*, 47(29):5394–5399.
- Isoz, W., Svensson, T., and Renhorn, I. (2005). Nonuniformity correction of infrared focal plane arrays.
- Jonah C. McBride, M. S. S. (2009). Improving scene-based nonuniformity correction for infrared images using frequency domain processing.
- Kai, M., Zhan, S., Xiaodong, P., Yongsheng, W., and Wenbin, L. (2016). An interpolation method based on two-step approach model for bad point in bayer color image. In *2016 2nd IEEE International Conference on Computer and Communications (ICCC)*, pages 599–602.
- Kumar, A. (2013). Sensor non uniformity correction algorithms and its real time implementation for infrared focal plane array-based thermal imaging system. *Defence Science Journal*, 63(6):589–598.
- Liang, C., Sang, H., and Shen, X. (2014). Efficient scene-based method for real-time non-uniformity correction of infrared video sequences. *Electronics Letters*, 50(12):868–870.
- Lin, Y. and Calarco, A. (1990). Offset, gain and bad pixel correction in electronic scanning arrays. US Patent 4,920,428.
- Milton, A. F., Barone, F. R., and Kruer, M. R. (1985). Influence of nonuniformity on infrared focal plane array performance. *Optical Engineering*, 24:24 – 24 – 8.
- Ness, G., Oved, A., and Kakon, I. (2017). Derivative based focal plane array nonuniformity correction. *CoRR*, abs/1702.06118.
- Schulz, M. and Caldwell, L. (1995). Nonuniformity correction and correctability of infrared focal plane arrays. *Infrared Physics & Technology*, 36(4):763 – 777.
- Shi, H., Zhang, Q., Qian, J., Mao, L., Cheng, T., Gao, J., Wu, X., Chen, D., and Jiao, B. (2009). Optical sensitivity analysis of deformed mirrors for microcantilever array ir imaging. *Opt. Express*, 17(6):4367–4381.
- Vera, E., Meza, P., and Torres, S. (2011). Total variation approach for adaptive nonuniformity correction in focal-plane arrays. *Opt. Lett.*, 36(2):172–174.
- Wang, M., Tsukamoto, T., and Tanaka, S. (2015). Uncooled infrared thermal imaging sensor using vacuum-evaporated europium phosphor. *Journal of Micromechanics and Microengineering*, 25(8):085001.
- Young, S. S., Driggers, R. G., and Jacobs, E. L. (2008). *Signal Processing and Performance Analysis for Imaging Systems*. Artech House, Inc., Norwood, MA, USA.
- Yuan, X., Wan, W., and Zhao, M. (1995). New method for nonuniformity correction of solid state image sensor. *Proc.SPIE*.